Hindawi
Journal of Nanomaterials
Volume 2019, Article ID 8175803, 8 pages
https://doi.org/10.1155/2019/8175803

Research Article

Preparation of Ag-Coated SiO_2@TiO_2 Core-Shell Nanocomposites and Their Photocatalytic Applications towards Phenol and Methylene Blue Degradation

Ning Fu,[1,2] **Xue-chang Ren**,[1] **and Jian-xin Wan**[1]

[1]*School of Environmental & Municipal Engineering, Lanzhou Jiaotong University, Lanzhou 730070, China*
[2]*Gansu Environmental Monitoring Center, Lanzhou 730020, China*

Correspondence should be addressed to Xue-chang Ren; rxchang1698@hotmail.com

Received 2 July 2019; Accepted 24 August 2019; Published 15 October 2019

Guest Editor: Fei Ke

Ag-coated SiO_2@TiO_2 (Ag-SiO_2@TiO_2) core-shell nanocomposites were synthesized by a two-step method, which combined hydrothermal process and photodeposition. The morphology, structure, composition, and optical properties of the Ag-coated SiO_2@TiO_2 nanocomposites were extensively characterized by field-emission scanning microscopy (FE-SEM), transmission electron microscopy (TEM), energy-dispersive X-ray spectroscopy (EDS), X-ray diffraction (XRD), X-ray photoelectron spectroscopy (XPS), and Fourier-transform infrared spectra (FT-IR spectra). The anatase TiO_2 nanoparticles (5-10 nm) with high surface area were loaded on SiO_2 spheres (200-300 nm) in the form of SiO_2@TiO_2 core-shell nanoparticle with a porous shell of controlled thickness (10–30 nm). Ag nanoparticles of different mass concentrations were photodeposited on SiO_2@TiO_2 core-shell structure with particle sizes of about 10-20 nm. The results showed that Ag nanoparticles increased the photocatalytic activity of SiO_2@TiO_2 core-shell nanoparticle improved the degradation of phenol and methylene blue under UV irradiation. The experimental results showed that Ag nanoparticles with mass concentrations of 6% had the highest photocatalytic activity on SiO_2@TiO_2 core-shell nanoparticles.

1. Introduction

Titanium dioxide (TiO_2), because of its high chemical stability, easy availability, and nontoxicity, is one of the most important semiconductor photocatalysts [1–3]. Using of high surface area TiO_2 as a photocatalyst for the degradation of contaminants has attracted intense attention and has been widely used [4–6]. However, the degradation efficiency of TiO_2 is restricted by the large bandgap (3.2 eV) and the high recombination rate of photogenerated electron-hole pairs tend to reduce the full use of UV and solar energy [7–9]. Besides, it is difficult to recycle the TiO_2 particles from solution after photodegradation. In order to eliminate these obstacles, larger SiO_2 particles were chosen as the carrier for the dispersion of TiO_2 nanoparticles due to its thermal stability, high chemical inertia, large specific surface area, and high adsorption, which are beneficial to the interfacial reaction of the composite material [10–12]. Compared with TiO_2 catalyst, SiO_2@TiO_2 core-shell nanoparticles have good photocatalytic activity as photocatalyst [13, 14].

Noble metals such as Ag, Au, and Pt were deposited on the surface of TiO_2 nanoparticles, thereby suppressing the recombination of electron-hole pairs, prolonging the lifetime of the electron-hole pairs and improving its degradation efficiency [15–19]. Among noble metals, Ag has been proved as an effective doping metal on the surface of TiO_2 nanoparticles to improve photocatalytic efficiency due to its high work function and its ability to generated surface plasmons at desired wavelengths [20]. In addition, Ag is not only easy to attach to the surface of SiO_2@TiO_2 spheres but also stable and easily available [21–25].

Previous studies on Ag-TiO_2-SiO_2 photocatalysts mostly deposited Ag nanoparticles on agglomerated SiO_2/TiO_2 nanocomposites with irregular shape and size [26–28], ignoring Ag-TiO_2-SiO_2 nanoparticles with uniform shape and size [29–31]. Besides, few studies focused on the degradation

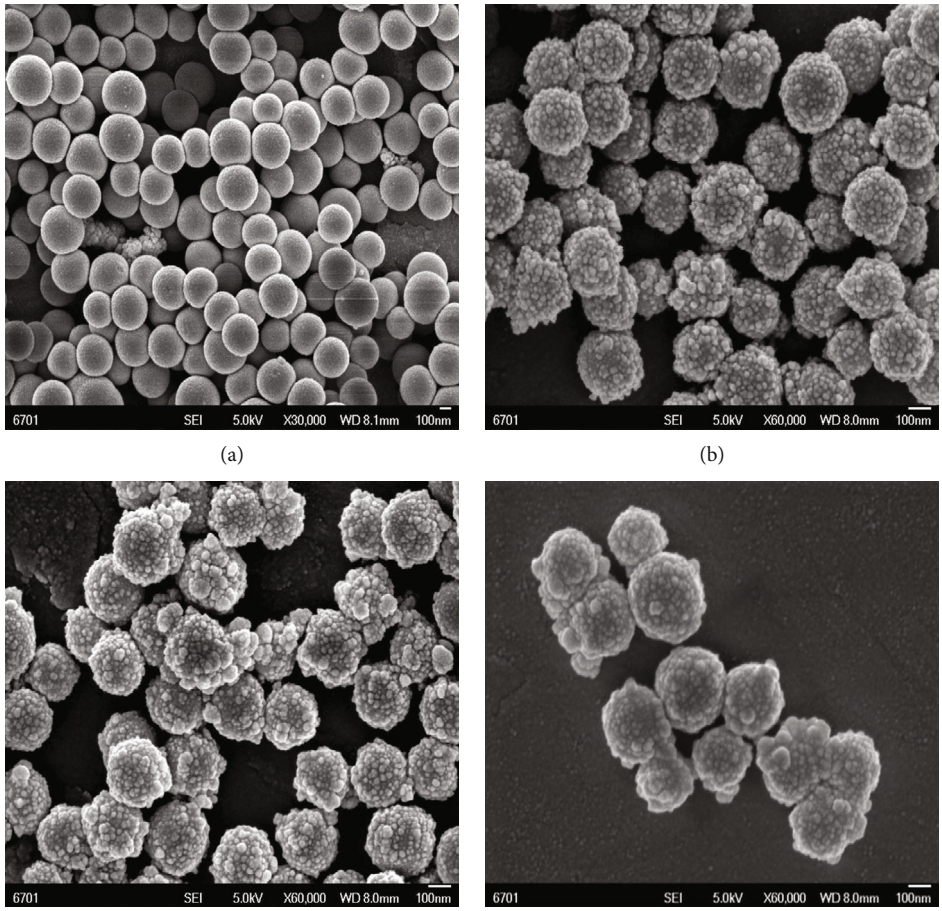

Figure 1: SEM images of (a) SiO_2, (b) SiO_2@TiO_2 core-shell particles, and (c, d) 6 wt.% Ag-coated SiO_2@TiO_2.

substrates towards both colorless organic matters (such as phenol) and colored organic dyes (such as methylene blue) with higher photocatalytic efficiency.

Here, the TiO_2 nanoparticles were coated on the SiO_2 spheres by hydrothermal method using SiO_2 as core to increase the surface area. Further, Ag-coated SiO_2@TiO_2 nanocomposites were synthesized by photodeposited Ag nanoparticles on the SiO_2@TiO_2 composite spheres with uniformity in size and shape. The surface morphology of the Ag-coated SiO_2@TiO_2 nanocomposite was investigated by transmission electron microscopy (TEM) and scanning electron microscopy (SEM). The photocatalytic activity toward the degradation of phenol and methylene blue under UV light was tested.

2. Experimental

2.1. Chemicals. In this study, analytical-grade chemicals were used without further purification. Tetraethyl orthosilicate (TEOS; 99.9%) was purchased from XiYa Reagent company, titanium (IV) isopropoxide (TTIP; 95%) was obtained from Sigma-Aldrich, silver nitrate ($AgNO_3 \cdot 6H_2O$; 99%), isopropanol, ethanol, NH_4OH (25%), sodium bromide, phenol, and methylene blue (MB) were manufactured by Sinopharm Chemical Reagent company.

2.2. Synthesis of SiO_2 Spheres. The SiO_2 spheres were prepared according to the literature [30]. Typically, 15 mL H_2O and 4 mL NH_4OH (25%) were added to 100 mL ethanol in a Teflon reactor and left under magnetic stirring for 30 min. Then, 3.0 mL of TEOS was quickly added to the above mixture and stirred at room temperature ($25 \pm 2^{\circ}C$) for 3 h. Then, the mixture was neutralized with 5 mol L^{-1} HCl and centrifuged at 4000 rpm for 10 min. The SiO_2 spheres were separated by centrifugation and washed four times with ethanol and distilled water. The resulting precipitate was dried at 70°C for at least 20 h to obtain SiO_2 spheres.

2.3. Synthesis of SiO_2@TiO_2 Core-Shell Nanoparticles. The SiO_2@TiO_2 core-shell nanoparticles were also fabricated according to the literatures with minor modifications [30]. The synthesis process is as follows: 1.0 g SiO_2 powder was dried at 110°C for 1 h and then sonicated in 80 mL isopropanol for 1 h. Then, 1.0 mL titanium isopropoxide (TTIP) was quickly added and kept under magnetic stirring for 24 h. Subsequently, 15 mL water–alcohol mixture (5 mL H_2O : 10 mL isopropanol) was slowly added (2 mL min^{-1}) and magnetically stirred for 3 h. The resulting precipitate was washed once with isopropanol and subsequently twice with deionized water at 8000 rpm. The amorphous TiO_2 shell was crystallized by hydrothermal treatment. The resulting

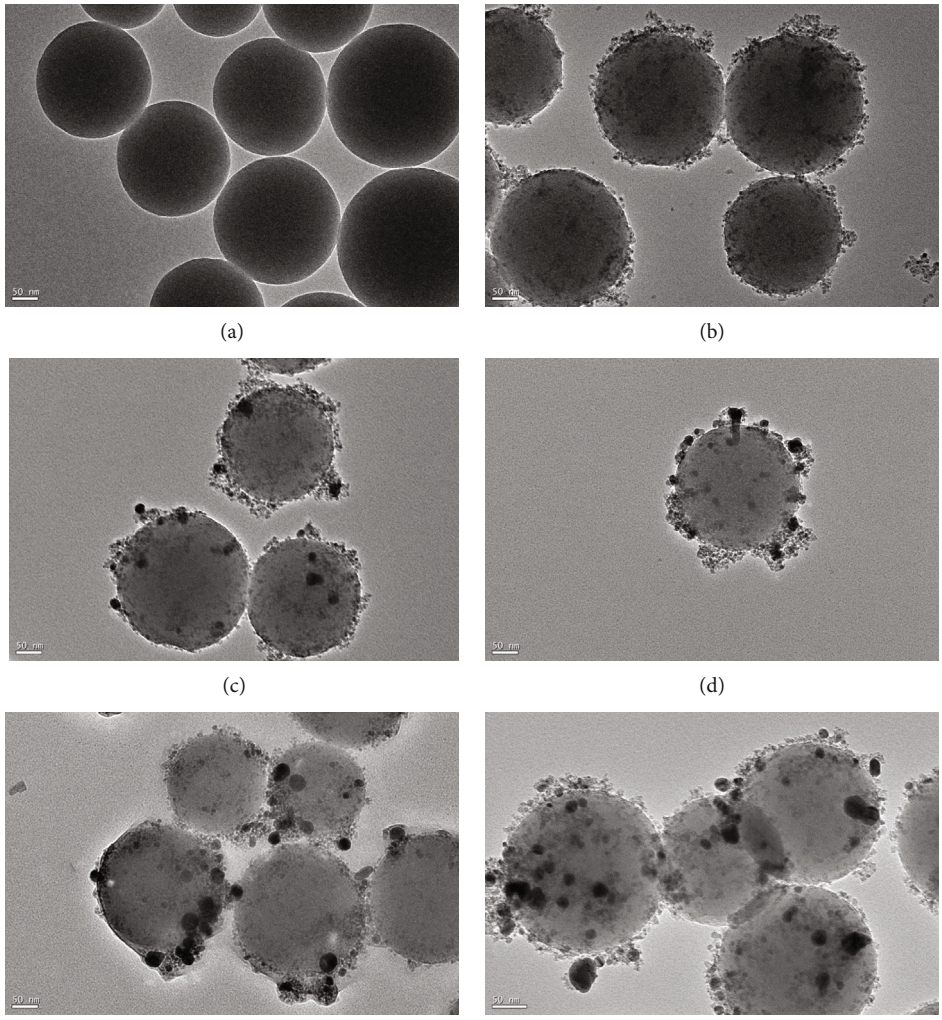

Figure 2: TEM images of (a) SiO_2, (b) SiO_2@TiO_2 core-shell particles, (c) 1 wt.% Ag-coated SiO_2@TiO_2 photocatalysts, (d) 3 wt.% Ag-coated SiO_2@TiO_2 photocatalysts, (e) 6 wt.% Ag-coated SiO_2@TiO_2 photocatalysts, and (f) 9 wt.% Ag-coated SiO_2@TiO_2 photocatalysts.

amorphous SiO_2@TiO_2 core-shell nanoparticles were suspended in 50 mL H_2O, treated at 105°C for 24 h, and then centrifuged again at 8000 rpm for 10 min. The obtained precipitate was dried at 70°C for 20 h, and finally calcined at 450°C for 2 h. The unsupported TiO_2 was also prepared using 3 mL of TTIP by the same procedure used for the preparation of SiO_2@TiO_2 core-shell nanoparticles but in the absence of SiO_2 in the reaction mixture.

2.4. Synthesis Ag-Coated SiO_2@TiO_2 Core-Shell Nanoparticles. Different concentrations of Ag particles were deposited on SiO_2@TiO_2 core-shell nanoparticles by photodeposition. 0.2 g SiO_2@TiO_2 composite spheres were dispersed by ultrasonication in 80 mL ethanol for 1 h. 0.340 g silver nitrate was dissolved in 50 mL deionized water with the concentration of 2 mM. The various amounts of silver nitrate were then added into the suspension of SiO_2@TiO_2 core-shell nanoparticles such that the Ag^+ concentration was maintained at 1, 3, 6, and 9 wt.% relative to the SiO_2@TiO_2. The above solution mixtures were then placed under a high-pressure Hg UV lamp for 60 min to deposit Ag^+ light on the SiO_2@TiO_2 composite spheres. The precipitate was obtained by centrifugation, and then sodium bromide was added to the supernatant to detect the presence of silver bromide to determine whether or not free "Ag" ions were present. The results confirmed that silver ions were deposited on the surface of SiO_2@TiO_2 core-shell nanoparticles. Finally, the resulting precipitate was washed with ethanol and dried at 70°C for 24 h.

2.5. Materials Characterization. The crystal phase of the as-prepared samples was determined by X-ray diffraction (XRD) using Cu-Kα radiation ($\lambda = 1.5418$°A). Fourier-transform infrared (FT-IR) spectra of the samples were evaluated by an IR Prestige-21 FT-IR spectrometer (Shimadzu, Japan) using the conventional KBr pellet method. A PHI-5702 multifunctional X-ray photoelectron spectroscope (XPS) was used to analyze the chemical state of Ag on the TiO_2 surface, using Mg Ka radiation as the excitation source and the binding energy of contaminated carbon (C1s: 285 eV) as the reference. The surface morphology was examined by SEM (JSM-6701F, Japan) and TEM (Tecnai G^2,

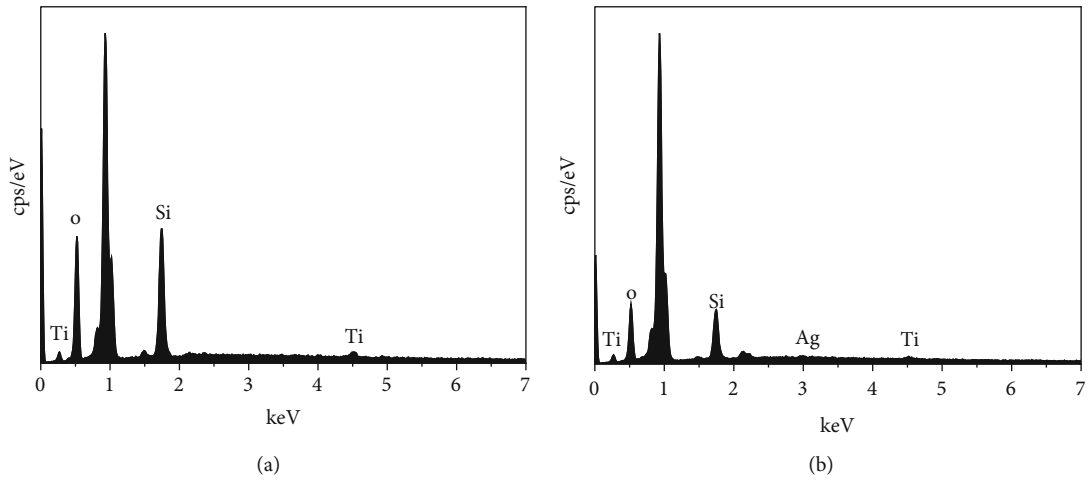

Figure 3: EDS spectrum of (a) SiO_2@TiO_2 core-shell particles and (b) 6 wt.% Ag-SiO_2@TiO_2 nanocomposite spheres.

American). The degradation of phenol and MB was monitored by a 3100 UV spectrophotometer.

2.6. Photodegradation Experiments. The photocatalytic activity of the samples were evaluated by the photodegradation of phenol and MB in a reactor using a 500 W high-pressure mercury lamp. In each experiment, 75 mg of prepared photocatalysts and 300 mL of an aqueous solution of phenol or MB having an initial concentration of 20 mg/L were dispersed in the substrate solution. In order to ensure the adsorption and desorption equilibrium between the photocatalyst and substrates, the reaction solutions were carried out under UV light after stirring for 30 minutes in the dark. 4 mL of the suspension was collected from the reactor at different irradiation time intervals and centrifuged to remove the photocatalyst completely. The concentration changes of MB were analyzed by recording the maximum absorbance of MB at 664 nm, and the phenol was analyzed by colorimetric method of 4-aminoantipyrine at 510 nm.

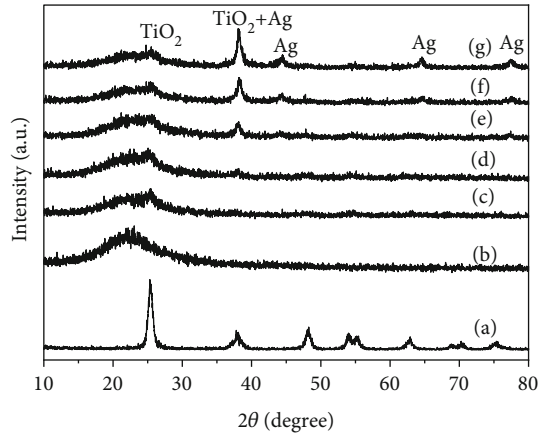

Figure 4: XRD patterns of (a) TiO_2, (b) SiO_2, (c) SiO_2@TiO_2 core-shell particles, (d) 1 wt.% Ag-coated SiO_2@TiO_2 photocatalysts, (e) 3 wt.% Ag-coated SiO_2@TiO_2 photocatalysts, (f) 6 wt.% Ag-coated SiO_2@TiO_2 photocatalysts, and (g) 9 wt.% Ag-coated SiO_2@TiO_2 photocatalysts.

3. Results and Discussion

3.1. Synthesis and Morphological Characterization. The morphology and structure of Ag-coated SiO_2@TiO_2 photocatalysts were characterized by SEM and TEM. As shown in Figure 1(a), the SiO_2 core was a smooth spherical particle of about 200-300 nm. As shown in Figure 1(b), the SiO_2@TiO_2 core-shell particles still kept spherical structure compared with SiO_2 spheres, but the surface appears rough and textured due to the amount of TiO_2 nanoparticles deposited on the SiO_2 spheres. The average SiO_2@TiO_2 core-shell particles size was 210-330 nm, and the coating small TiO_2 particles with the size of about 5~10 nm aggregated on the surface of SiO_2 spheres after annealing at 450°C for 2 h. Figures 1(c) and 1(d) show the SEM images of 6 wt.% Ag-coated SiO_2@TiO_2 photocatalysts; it was difficult to distinguish the photodeposited Ag nanoparticles on SiO_2@TiO_2 composite spheres for aggregating together with TiO_2 nanoparticles.

The TEM images of SiO_2 core spheres and SiO_2@TiO_2 core-shell particles in Figures 2(a) and 2(b) showed the same morphology and structure with the SEM images. Figures 2(c)–2(f) show TEM images of the 1, 3, 6, and 9 wt.% (initial concentration) Ag nanoparticles photodeposited on SiO_2@TiO_2 composite spheres and also show the morphology of photodeposited Ag nanoparticles. The size and density of the Ag nanoparticles increased as the initial concentration of $AgNO_3$ increased.

The EDS spectrum of the SiO_2@TiO_2 composite spheres and the 6 wt.% Ag-coated SiO_2@TiO_2 nanocomposites are shown in Figures 3(a) and 3(b). At the same time, the EDS analysis also confirmed that Si and Ti and O peaks were present in the SiO_2@TiO_2 composite spheres (Figure 3(a)). The presence of Ag nanoparticles was confirmed by EDS in Ag-coated SiO_2@TiO_2 photocatalysts as shown in Figure 3(b).

3.2. XRD Analysis. The XRD patterns of the synthesized TiO_2, SiO_2, SiO_2@TiO_2, and Ag-coated SiO_2@TiO_2 photocatalysts are shown in Figure 4. As shown in Figure 4(a), the

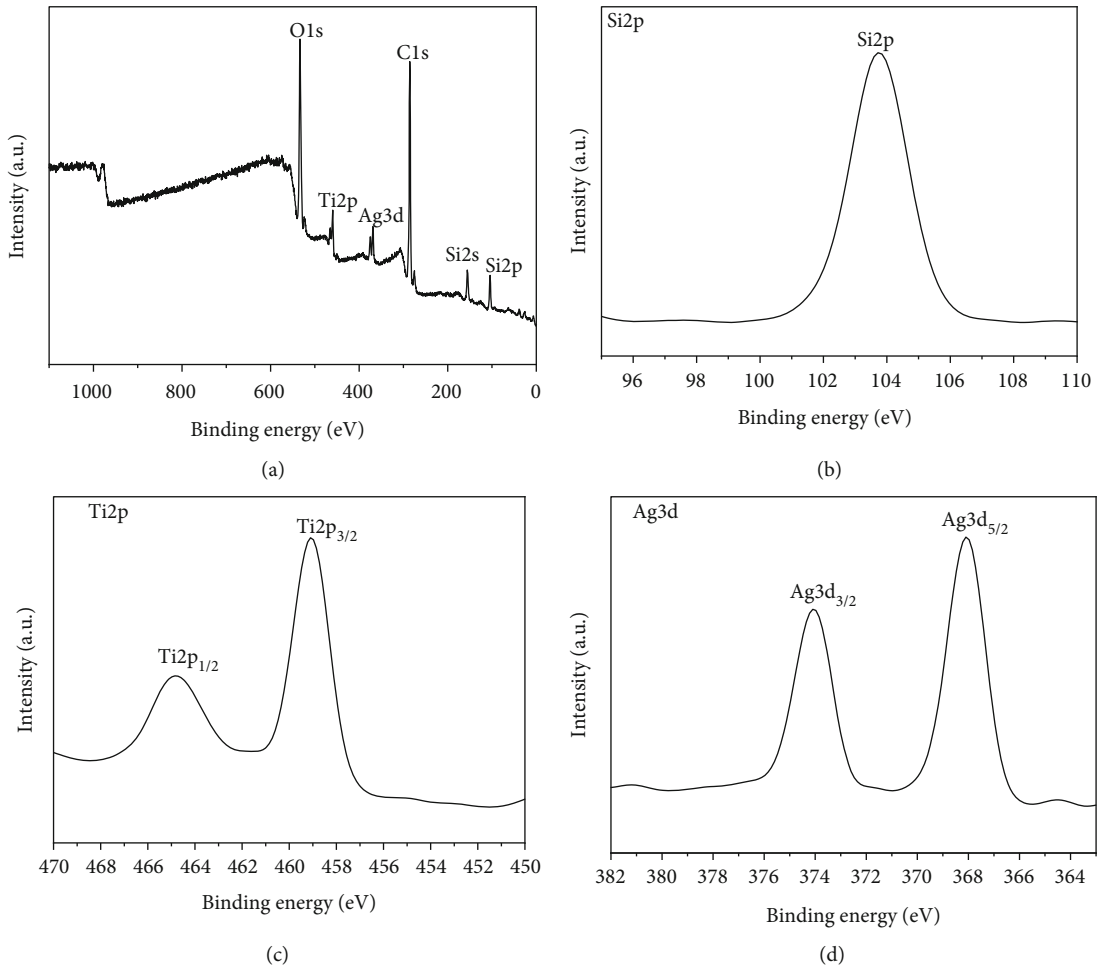

Figure 5: XPS spectra of 6 wt.% Ag-coated SiO_2@TiO_2 photocatalysts: survey (a), high-resolution Si 2p (b), Ti 2p (c), and Ag 3d (d).

obvious diffraction peaks at $2\theta = 25.3^\circ$, 37.8°, 48.2°, 54°, and 62.9° corresponded to (101), (004), (200), (211), and (204) crystal planes of anatase TiO_2, respectively [27]. The wide diffraction peak at $2\theta = 23^\circ$ was ascribed to the amorphous SiO_2 in Figure 4(b). No characteristic anatase TiO_2 diffraction peaks occurred in the SiO_2@TiO_2 precursor spheres after the deposition of TiO_2 because of more SiO_2 amorphous structure in Figure 4(c). After photodeposition of Ag on SiO_2@TiO_2, new peaks appeared at 38°, 44.1°, 64.6°, and 77° that corresponded to the (111), (200), (220), and (311) diffraction planes of face-centered cubic Ag crystal (PDF#65-2871), respectively [32]. Meanwhile, the peak intensity of Ag significantly enhanced because the Ag weight increased as shown in Figures 4(d)–4(g).

3.3. XPS Analysis. X-ray photoelectron spectroscopy (XPS) was used to analyze the surface compositions and chemical states of the Si, Ti, and Ag elements in the 6 wt.% Ag-coated SiO_2@TiO_2 nanocomposites as shown in Figure 5. As shown in Figure 5(a), four elements of Ag, O, Si, and Ti appeared in the measured spectrum, indicating that Ag successfully adhered to the surface of SiO_2@TiO_2. The binding energy peaks of Si, Ti, and Ag are shown in Figures 5(b)–5(d), respectively. The binding energy of Si 2p XPS spectrum

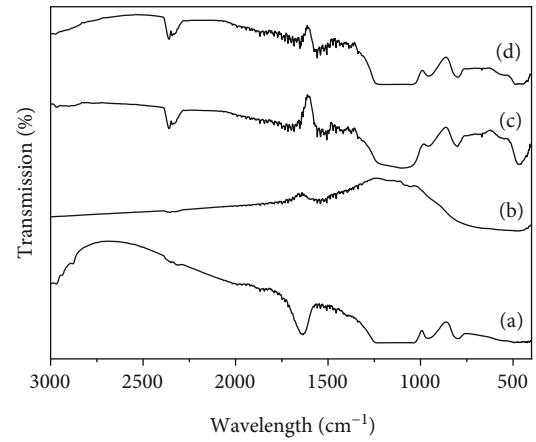

Figure 6: FT-IR spectra of (a) SiO_2, (b) TiO_2, (c) SiO_2@TiO_2, and (d) 6 wt.% Ag-coated SiO_2@TiO_2.

(Figure 5(b)) at 103.7 eV indicated the formation of a Si-O-Si bond. The binding energy of Ti 2p XPS spectrum (Figure 5(c)) showed at 464.7 and 459.0 eV corresponds to Ti $2p_{1/2}$ and Ti $2p_{3/2}$, respectively. This result confirmed the formation of pure anatase TiO_2. The binding energy of Ag 3d appeared at 368.1 eV and 374.1 eV which corresponded

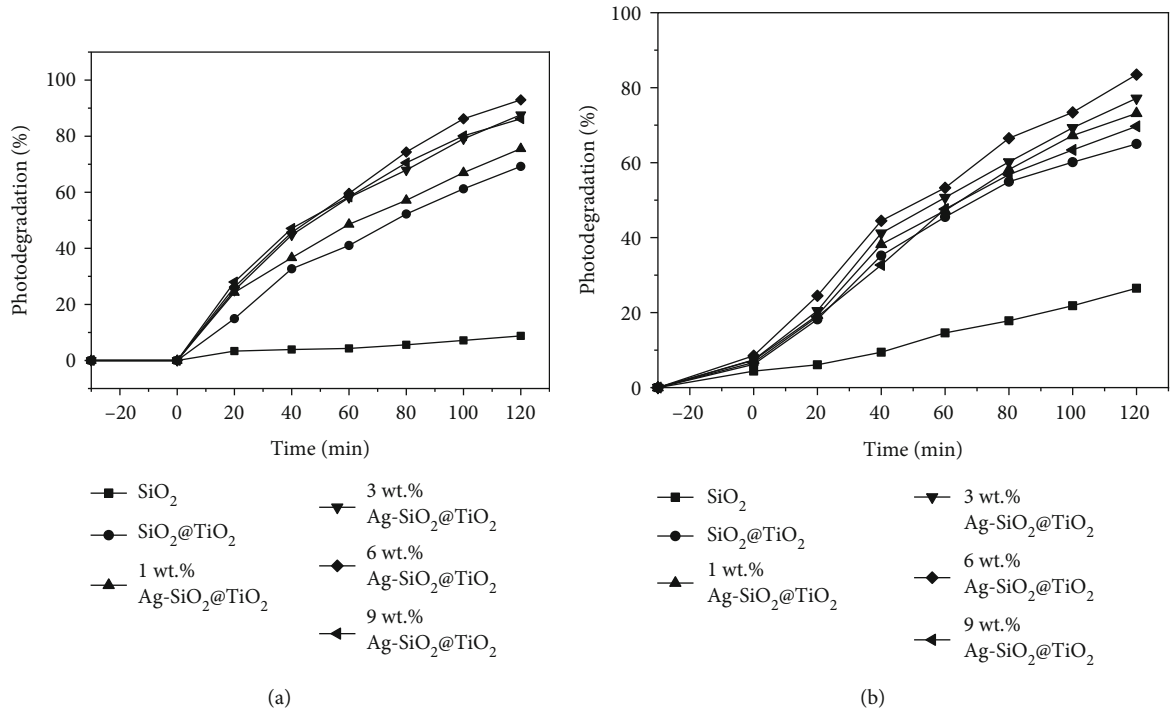

Figure 7: Photodegradation of phenol (a) and methylene blue (b) under UV light: SiO_2, SiO_2@TiO_2, and Ag-coated SiO_2@TiO_2.

to the Ag $3d_{5/2}$ and Ag $3d_{3/2}$ orbits, respectively, as shown in Figure 2(b), and the splitting of the 3d doublet was 6.0 eV. The results indicated that Ag presented in the composites in the form of metallic Ag. This result was in good agreement as well with standard binding energy value of metallic silver (Ag^0) present in the SiO_2@TiO_2 composite spheres [32–34]. According to the results of XRD patterns, it can be concluded that Ag particles were not oxidized in the process of preparation under UV irradiation.

3.4. FT-IR Spectra Analysis. FT-IR spectra were performed to analyze the composition of SiO_2, TiO_2, SiO_2@TiO_2, and 6 wt.% Ag-coated SiO_2@TiO_2. As shown in Figure 6, the bands at 800 cm^{-1} were ascribed to the symmetric stretching vibration of Si-O-Si (Figure 6(a)) [35]; the peaks around 470 cm^{-1} were attributed to the Ti-O-Ti vibration in TiO_2 (Figure 6(b)). For SiO_2@TiO_2 and Ag-coated SiO_2@TiO_2, the peaks at 955 cm^{-1} and 1053 cm^{-1} were assigned to the asymmetric vibration of Ti-O-Si (Figures 6(a)–6(d)) [36].

3.5. Photocatalytic Activity. Figure 7 shows the photocatalytic activity of phenol (Figure 7(a)) and MB (Figure 7(b)) in the presence of SiO_2, SiO_2@TiO_2, and Ag-coated SiO_2@TiO_2, respectively. As shown in Figure 7(a), SiO_2 had only 8.78% photocatalytic efficiency after 120 min photodegration of phenol which was attributed to the adsorption of SiO_2. It can be clearly seen that the photocatalytic efficiency of Ag-coated SiO_2@TiO_2 showed more excellent activity than SiO_2@TiO_2 microspheres. The results indicated that among the different weights of Ag-coated SiO_2@TiO_2 photocatalysts, 6 wt.% Ag-coated SiO_2@TiO_2 photocatalysts showed the highest photocatalytic efficiency of 92.9%. From Figure 7(b), the photocatalytic efficiency of SiO_2, SiO_2@TiO_2, and Ag-coated SiO_2@TiO_2 towards MB at the wavelength of 664 nm showed the same photocatalytic regulation of photodegration of phenol under UV irradiation. SiO_2 showed more photocatalytic efficiency of 26.5% after 120 min photodegration of MB than the photodegration of phenol which indicated that SiO_2 had more adsorption efficiency towards colored dye than colorless organic matters on the surface or inside of the SiO_2 spheres. The results also showed that Ag-coated SiO_2@TiO_2 exhibited higher photocatalytic efficiency than SiO_2 and SiO_2@TiO_2, and 6 wt.% Ag-coated SiO_2@TiO_2 photocatalysts presented the highest photocatalytic efficiency of 83.5%. The more excellent photocatalytic activity of Ag-coated SiO_2@TiO_2 may be caused by the smaller particle size and the higher concentration of catalytically active centers of the anatase nanocrystals in the calcined TiO_2 shell than in the calcined solid TiO_2 sphere [37, 38]. Besides, the Ag nanoparticles helped suppress the regeneration of the electron-hole recombination of the semiconductor (TiO_2). Obviously, in the Ag-coated SiO_2@TiO_2 photocatalytic system, SiO_2 acted as the adsorbent, while TiO_2 acted as the photoactive center, and Ag acted as an electron trapping agent [37].

4. Conclusions

Ag-coated SiO_2@TiO_2 core-shell nanocomposites were synthesized by a two-step hydrothermal and photodeposition method. The samples were characterized by TEM and other methods. The results showed that Ag nanoparticles were deposited on the SiO_2@TiO_2 composite spheres with good dispersibility and no aggregation. The XRD profiles showed the presence of anatase phase in TiO_2 and the XPS results indicated that Ag existed in the form of metallic Ag in the Ag-coated SiO_2@TiO_2 composite sphere. FT-IR spectra

results showed that the asymmetric vibration of Ti-O-Si presented in the Ag-coated SiO_2@TiO_2 composite sphere. Compared with the SiO_2@TiO_2 composite spherical photocatalyst, the Ag-coated SiO_2@TiO_2 composite sphere had better catalytic activity for the degradation of phenol and MB under UV light irradiation.

Data Availability

The data used to support the findings of this study are available from the corresponding author upon request.

Conflicts of Interest

The authors declare that there is no conflict of interests regarding the publication of this paper.

Acknowledgments

The authors would like to thank the financial support from the National Natural Science Foundation of China (NSFC no. 51268026).

References

[1] A. Fujishima and K. Honda, "Electrochemical photolysis of water at a semiconductor electrode," *Nature*, vol. 238, no. 7, pp. 37-38, 1972.

[2] N. S. Waldmann and Y. Paz, "Away from TiO_2: a critical mini-review on the developing of new photocatalysts for degradation of contaminants in water," *Materials Science in Semiconductor Processing*, vol. 42, no. 6, pp. 72–80, 2016.

[3] H. Zangeneh, A. A. L. Zinatizadeh, M. Habibi, M. Akia, and M. H. Isa, "Photocatalytic oxidation of organic dyes and pollutants in wastewater using different modified titanium dioxides: a comparative review," *Journal of Industrial and Engineering Chemistry*, vol. 26, no. 10, pp. 1–36, 2015.

[4] E. B. Moushoul, Y. Mansourpanah, K. Farhadi, and M. Tabatabaei, "TiO_2 nanocomposite based polymeric membranes: a review on performance improvement for various applications in chemical engineering processes," *Chemical Engineering Journal*, vol. 283, no. 124, pp. 29–46, 2016.

[5] B. Szczepanik, "Photocatalytic degradation of organic contaminants over clay-TiO_2 nanocomposites: a review," *Applied Clay Science*, vol. 141, no. 29, pp. 227–239, 2017.

[6] E. Grabowska, J. Reszczyńska, and A. Zaleska, "RETRACTED:Mechanism of phenol photodegradation in the presence of pure and modified-TiO_2: a review," *Water Research*, vol. 46, no. 17, pp. 5453–5471, 2012.

[7] A. L. Linsebigler, G. Lu, and J. T. Yates Jr., "Photocatalysis on TiO2 surfaces: principles, mechanisms, and selected results," *Chemical Reviews*, vol. 95, no. 3, pp. 735–758, 2012.

[8] H. Xu, S. X. Ouyang, L. Q. Liu, P. Reunchan, N. Umezawa, and J. Ye, "Recent advances in TiO_2-based photocatalysis," *Journal of Materials Chemistry A*, vol. 2, no. 32, pp. 12642–12661, 2014.

[9] G. Liu, L. C. Yin, J. Wang et al., "A red anatase TiO_2 photocatalyst for solar energy conversion," *Energy & Environmental Science*, vol. 5, no. 11, pp. 9603–9610, 2014.

[10] I. Kitsou, P. Panagopoulos, T. Maggos, M. Arkas, and A. Tsetsekou, "Development of SiO_2@TiO_2 core-shell nanospheres for catalytic applications," *Applied Surface Science*, vol. 441, no. 5, pp. 223–231, 2018.

[11] L. H. Wu, Y. F. Zhou, W. Y. Nie, L. Song, and P. Chen, "Synthesis of highly monodispersed teardrop-shaped core-shell SiO_2/TiO_2 nanoparticles and their photocatalytic activities," *Applied Surface Science*, vol. 351, no. 5, pp. 320–326, 2015.

[12] W. Li, J. P. Yang, Z. X. Wu et al., "A versatile kinetics-controlled coating method to construct uniform porous TiO_2 shells for multifunctional core–shell structures," *Journal of the American Chemical Society*, vol. 134, no. 29, pp. 11864–11867, 2012.

[13] J. W. Lee, M. R. Othman, Y. Eomc, T. G. Lee, W. S. Kim, and J. Kim, "The effects of sonification and TiO_2 deposition on the micro-characteristics of the thermally treated SiO_2/TiO_2 spherical core–shell particles for photo-catalysis of methyl orange," *Microporous and Mesoporous Materials*, vol. 116, no. 1-3, pp. 561–568, 2008.

[14] C. Anderson and A. J. Bard, "An improved photocatalyst of TiO2/SiO2 prepared by a Sol-gel synthesis," *The Journal of Chemical Physics*, vol. 99, no. 24, pp. 9882–9885, 1995.

[15] T. Okuno, G. Kawamuran, H. Muto, and A. Matsuda, "Photocatalytic properties of Au-deposited mesoporous SiO_2–TiO_2 photocatalyst under simultaneous irradiation of UV and visible light," *Journal of Solid State Chemistry*, vol. 235, no. 12, pp. 132–138, 2016.

[16] L. X. Zhang, C. H. Ni, H. F. Jiu, C. Xie, J. Yan, and G. Qi, "One-pot synthesis of Ag-TiO_2/reduced graphene oxide nanocomposite for high performance of adsorption and photocatalysis," *Ceramics International*, vol. 43, no. 7, pp. 5450–5456, 2017.

[17] R. Kaur and B. Pal, "Size and shape dependent attachments of Au nanostructures to TiO_2 for optimum reactivity of Au–TiO_2 photocatalysis," *Journal of Molecular Catalysis A: Chemical*, vol. 355, no. 11, pp. 39–43, 2012.

[18] Z. Zheng, B. Huang, X. Qin, X. Zhang, Y. Dai, and M.-H. Whangbo, "Facile *in situ* synthesis of visible-light plasmonic photocatalysts M@TiO_2 (M = Au, Pt, Ag) and evaluation of their photocatalytic oxidation of benzene to phenol," *Journal of Materials Chemistry*, vol. 21, no. 11, pp. 9079–9087, 2011.

[19] D. Y. Zhou, Y. M. Liu, W. G. Zhang, W. Liang, and F. Yang, "Au-TiO_2 nanofilms for enhanced photocatalytic activity," *Thin Solid Films*, vol. 636, no. 11, pp. 490–498, 2017.

[20] H. Eskandarloo, A. Badiei, M. A. Behnajady, and M. Afshar, "Enhanced photocatalytic removal of phenazopyridine by using silver-impregnated SiO_2–TiO_2 nanoparticles: optimization of synthesis variables," *Research on Chemical Intermediates*, vol. 41, no. 12, pp. 9929–9949, 2015.

[21] H. M. S. Suh, J. R. Choi, H. J. Hah, S. M. Koo, and Y. C. Bae, "Comparison of Ag deposition effects on the photocatalytic activity of nanoparticulate TiO_2 under visible and UV light irradiation," *Journal of Photochemistry and Photobiology A: Chemistry*, vol. 163, no. 1-3, pp. 37–44, 2004.

[22] J. X. Li, J. H. Xu, W. L. Dai, and K. Fan, "Dependence of Ag deposition methods on the photocatalytic activity and surface state of TiO_2 with twistlike helix structure," *Journal of Physical Chemistry C*, vol. 113, no. 19, pp. 8343–83449, 2009.

[23] R. M. Mohamed and I. A. Mkhalid, "Characterization and catalytic properties of nano-sized Ag metal catalyst on TiO_2–SiO_2 synthesized by photo-assisted deposition and impregnation methods," *Journal of Alloys and Compounds*, vol. 501, no. 2, pp. 301–306, 2010.

[24] B. Braconnier, C. A. Páez, S. Lambert et al., "Ag- and SiO_2-doped porous TiO_2 with enhanced thermal stability," *Microporous and Mesoporous Materials*, vol. 122, no. 1-3, pp. 247–254, 2009.

[25] S. C. Chan and M. A. Barteau, "Preparation of highly uniform Ag/TiO_2 and Au/TiO_2 supported nanoparticle catalysts by photodeposition," *Langmuir*, vol. 21, no. 12, pp. 5588–5595, 2005.

[26] K. P. O. Mahesh, D. H. Kuo, and B. R. Huang, "Facile synthesis of heterostructured Ag-deposited SiO2@TiO2 composite spheres with enhanced catalytic activity towards the photodegradation of AB 1 dye," *Journal of Molecular Catalysis A: Chemical*, vol. 396, no. 10, pp. 290–296, 2015.

[27] X. Zhang, Y. Zhu, X. Yang et al., "Enhanced visible light photocatalytic activity of interlayer-isolated triplex $Ag@SiO_2@$-TiO_2 core–shell nanoparticles," *Nanoscale*, vol. 5, no. 8, pp. 3359–3366, 2013.

[28] W. Zhao, L. Feng, R. Yang, J. Zheng, and X. Li, "Synthesis, characterization, and photocatalytic properties of Ag modified hollow SiO_2/TiO_2 hybrid microspheres," *Applied Catalysis B: Environmental*, vol. 103, no. 1-2, pp. 181–189, 2011.

[29] J. Zhou, F. Ren, S. Zhang et al., "SiO_2–Ag–SiO_2–TiO_2 multi-shell structures: plasmon enhanced photocatalysts with wide-spectral-response," *Journal of Materials Chemistry A*, vol. 1, no. 42, pp. 13128–13138, 2013.

[30] S. Ullah, E. P. F. Neto, A. A. Pasa et al., "Enhanced photocatalytic properties of core@shell $SiO_2@TiO_2$ nanoparticles," *Applied Catalysis B: Environmental*, vol. 179, no. 5, pp. 333–343, 2015.

[31] J. Ma, X. Guo, H. Ge, G. Tian, and Q. Zhang, "Seed-mediated photodeposition route to Ag-decorated $SiO_2@TiO_2$ microspheres with ideal core-shell structure and enhanced photocatalytic activity," *Applied Surface Science*, vol. 434, no. 5, pp. 1007–1014, 2018.

[32] W. Q. Li, X. H. Xiao, A. L. Stepanov et al., "The ion implantation-induced properties of one-dimensional nanomaterials," *Nanoscale Research Letters*, vol. 8, no. 1, article 175, 2013.

[33] M. Diak, E. Grabowska, and A. Zalesk, "Synthesis, characterization and photocatalytic activity of noble metal-modified TiO_2 nanosheets with exposed {0 0 1} facets," *Applied Surface Science*, vol. 347, pp. 275–285, 2015.

[34] C. Liu, D. Yang, Y. Wang, J. Shi, and Z. Jiang, "Fabrication of antimicrobial bacterial cellulose–Ag/AgCl nanocomposite using bacteria as versatile biofactory," *Journal of Nanoparticle Research*, vol. 14, no. 8, article 1084, pp. 1-2, 2012.

[35] C. Liu, D. Yang, Y. Jiao, Y. Tian, Y. Wang, and Z. Jiang, "Biomimetic synthesis of TiO_2–SiO_2–Ag nanocomposites with enhanced visible-light photocatalytic activity," *ACS Applied Materials & Interfaces*, vol. 5, no. 9, pp. 3824–3832, 2013.

[36] B. Subash, B. Krishnakumar, M. Swaminathan, and M. Shanthi, "Highly efficient, solar active, and reusable photocatalyst: Zr-loaded Ag–ZnO for reactive red 120 dye degradation with synergistic effect and dye-sensitized mechanism," *Langmuir*, vol. 29, no. 3, pp. 939–949, 2013.

[37] Q. Zhang, I. Lee, J. I. B. Joo, F. Zaera, and Y. Yin, "Core–shell nanostructured catalysts," *Accounts of Chemical Research*, vol. 46, no. 8, pp. 1816–1824, 2013.

[38] W. Li and D. Zhao, "Extension of the Stöber method to construct mesoporous SiO_2 and TiO_2 shells for uniform multifunctional core–shell structures," *Advanced Materials*, vol. 25, no. 1, pp. 142–149, 2013.